JOURNAL OF THERMOPHYSICS AND HEAT TRANSFER
Vol. 20, No. 3, July–September 2006

Sensitivity of Water Condensation in a Supersonic Plume to the Nucleation Rate

Jiaqiang Zhong,* Michael I. Zeifman,† and Deborah A. Levin‡
Pennsylvania State University, University Park, Pennsylvania 16802

The direct simulation Monte Carlo (DSMC) method has recently been developed to simulate homogeneous water condensation in a free expansion rocket plume. A nucleation rate, based on the classical nucleation theory (CNT), was used in the DSMC simulation to predict initial nuclei in the condensation region. However, recent experimental research suggests that the CNT nucleation rate should be corrected and the magnitude of the correction is a function of the vapor temperature. Because the nucleation rate is one of the most important factors that impacts the accuracy of the numerical simulation results for a condensation plume, the impact is investigated of the corrected nucleation rate on cluster growth processes and flow macroparameters in an expanding flow using the DSMC method to model both the gas and condensate flow.

Nomenclature

A, B	=	constant
c	=	velocity
d	=	diameter
E	=	energy
i	=	number of atoms
J	=	nucleation rate
k	=	Boltzmann's constant
m	=	molecular mass
q	=	sticking probability
r	=	cluster radius
T	=	temperature
V	=	specific volume
We	=	Weber number
ρ	=	density, 1000 kg/m^3
σ	=	surface tension, 0.074 N/m, or collision cross section

Subscripts

CER	=	corrected nucleation value
CNT	=	classical nucleation value
c	=	cluster species
g	=	gas state
l	=	liquid state
r	=	relative value
ref	=	reference value
$*$	=	critical state

I. Introduction

WITH use of the Mir spacecraft as an observation platform, radiance data from the UV to the visible spectral region has been obtained from the Soyuz thruster. The experimental arrangement, the instrumentation, and the data have been discussed in detail in Ref. 1. Numerical investigations of UV radiation from the Soyuz plume have also been performed, and the simulations were found to overpredict the experimental data by approximately a factor of 5–70 for an altitude of 380 km (Ref. 2). The UV radiation source is mainly OH species, the dissociation product of water (H_2O) molecules during collision processes with oxygen (O) atoms. Note that species O is from the freestream, whereas H_2O is one of the unsymmetrical dimethyl hydrazine/N_2O_4 combustion products of the Soyuz engine. Thus, accurate prediction of H_2O distributions in the expanding plume would be a critical precondition to validate the experimental OH species UV radiation data.

It can be shown that water vapor in the Soyuz exhaust flow becomes saturated and even supersaturated during the expanding process; thus, water may condense into water clusters. The numerical work[2] neglected the possibility of water condensation process in the Soyuz plume, which could be the reason of overpredicted UV radiation data. It is known that in the absence of foreign nuclei, homogeneous condensation[3–5] may occur if supercritical embryos form due to a large degree of supersaturation. Once the condensation process begins, it transfers mass from and adds energy to the gas phase, resulting in changes of the flowfield.[6] The changes that occur in the flowfield may affect the observance of high-altitude rocket plumes as well as result in increased likelihood of plume contamination of spacecraft surfaces.

Condensation in freely expanding flows has been studied for many years. Here we mention only a few papers that deal with the modeling of condensation. Assuming a one-dimensional and steady-state nucleation process, Wu[7] predicted the onset of homogeneous water condensation in the exhaust plume of an Apollo engine. Perrell et al.[8] calculated the condensation in a hypersonic wind tunnel by using a finite volume method in an axisymmetric formulation and showed that the condensation affects the flow temperature, pressure, Mach number, and mass fraction of liquid. Masuda et al.[9] studied the effects of water vapor condensation in a chemical oxygen–iodine laser and compared the excitation efficiency of oxygen with and without condensation in a one-dimensional calculation.

Most of the papers to date examine the condensation process in ground-based facilities using continuum approaches. There are very few experimental and theoretical treatments, however, on the condensation in rocket plumes expanding into a rarefied atmosphere at high altitudes. The important feature of these plumes is the strong gradients, especially in the vicinity of the nozzle lip and in the side- and backflow of the plume. The flow is characterized by a strong nonequilibrium, and the continuum approach is not strictly applicable. The accurate modeling of such plumes may require another approach, for example, a particle simulation method.

The direct simulation Monte Carlo (DSMC) method,[10] a kinetic particle approach, has been justified and used in our previous work[11] to model the coupled nonequilibrium gas expansion and homogeneous water condensation in a rocket plume. To simulate the condensation coupled plume, both cluster particles and molecules are

Received 28 June 2005; revision received 24 August 2005; accepted for publication 25 August 2005.

*Graduate Student; currently Postdoctoral Student, Department of Aerospace Engineering. Student Member AIAA.

†Research Associate, Department of Aerospace Engineering. Member AIAA.

‡Associate Professor, Department of Aerospace Engineering. Associate Fellow AIAA.

represented by the simulated particles and microscopic models including nucleation, cluster-monomer sticking and nonsticking collision, and cluster evaporation model have been developed to describe interactions among cluster and gas molecules, based on the general momentum and energy conservation relationships. The developed DSMC condensation model was numerically validated by comparing simulation results with analytical solutions in one-dimensional test cases, further validated by comparison with Hagena's scaling laws (Hagena and Obert[12]), and finally applied to predict water homogeneous condensation in a rocket plume using classical nucleation rate. One of the important conclusions in the previous work[11] was that, based on the proposed microscopic models, the degree of condensation in a free-expanding plume is not sufficient to affect the flowfield.

However, the nucleation rate used in the previous work was taken from the classical nucleation theory (CNT).[3–5] Recent experimental research[13] suggests that the water classical nucleation rate should be corrected as a function of the vapor temperature. The nucleation rate determines the number of initial nuclei generated in a supersaturated plume and, therefore, greatly impacts the results of a condensation flow modeling. To accurately model the observed UV radiance data, it is important to study the impact of the nucleation rate correction on the Soyuz expanding plume. The paper is organized as follows. In Sec. II, we describe improvements to the previous developed microscopic models.[11] The results of the updated DSMC scheme for a rocket plume are discussed in detail in Sec. III. We find that the water number density in the condensation region is about 10–100 times less than the corresponding value of the flow without condensation, which may be the reason that the UV radiance in the Soyuz plume is overpredicted in Ref. 2.

II. Microscopic Models

The developed DSMC procedure involves the use of microscopic models that describe the interactions among clusters and gas molecules. These models include the nucleation model, the evaporation model, and the collision model.[11] In this section, we briefly review the improvements to the microscopic models. The detailed description of molecular dynamics simulation of cluster–monomer collisions may be found in Ref. 14 and cluster–cluster collisions in Ref. 15.

A. Cluster Model for Water

In a DSMC simulation, the simulated particle is usually assumed to be a spherical particle with a radius of r, and the number of collisions among simulated particles is calculated during each time step based on the collision cross section, $\sigma \approx \pi(r_1 + r_2)^2$, where subscripts 1 and 2 refer to the collision species. To simulate a condensation plume, in our previous work[11] we simply assumed that a radius r_i for the cluster consisting of i molecules is

$$r_i = i^{\frac{1}{3}} r_{\text{ref}} \tag{1}$$

where r_{ref} is the reference radius of the cluster molecule given in Ref. 10. Note that for small clusters[16] Eq. (1) may need to be corrected. A more accurate formula has been suggested in Ref. 17,

$$r_i = A i^{\frac{1}{3}} + B \tag{2}$$

where i is the number of molecules in the cluster and A and B are constants. Note that the improved definition of the cluster collision cross section obtained by using Eq. (2) instead of Eq. (1) is important for characterizing collisions between small clusters (such as a dimer and trimer) and monomers. Because the initial clusters in this work are created as clusters of critical size, according to the CNT, and cluster size can increase quickly through cluster–cluster coalescence processes, the impact of the new cluster model on the simulation results is not significant. However, for a future physically more plausible kinetic nucleation model that generates initial dimer clusters from triple collisions, the improvement of the cluster model may greatly affect the numerical results.

Molecular dynamics (MD) simulations can be used to validate these relationships. Unfortunately, the MD simulation of water is challenging due to multibody polarizable interactions indicating that two water molecules interact pairwise through nine electrostatic interactions, plus an additional Lennard–Jones potential acting between the molecular sites. Various potentials,[18] such as transferable intermolecular potentials 3 particles, transferable intermolecular potentials 4 particles, single point charge/extended single point charge, Carravetta and Clementi (C–C) (Ref. 19), and rigid polarized model (Ref. 20), have been suggested to simulate thermodynamic properties of water over a large range of temperature and pressure. More recently, Keutsch et al.[21] simulated water trimer cluster, Dang[22] simulated $(H_2O)_8$, $(H_2O)_9$, and $(H_2O)_{10}$ clusters, and Goldman and SayKally[23] simulated water clusters from dimer to $(H_2O)_6$. Because our goal is to estimate the parameters A and B in Eq. (2) rather than to characterize the full spectrum of cluster properties, we will use the available literature results to estimate A and B. Small water cluster radii[24] and large water cluster radii[25] are used for the estimation. By the choice of $A = 1.92$ and $B = 2.4$ Å, the MD simulation results of water cluster radii can be fitted well into Eq. (2). Thus, water cluster radius used in this work is calculated as $r_i = 1.92 i^{1/3} + 2.4$.

B. Nucleation Model

According to CNT,[3–5] initial clusters (nuclei) may be created in a supersaturated vapor environment. The nuclei are assumed to have the local critical size and to be in an equilibrium state with the surrounding gas. To implement the nucleation model in DSMC, we add a number of new simulated cluster particles into DSMC cells at each time step and remove the vapor molecules at the same time. The number of new cluster particles is defined by the nucleation rate, cell volume, and time step. The nucleation rate J_{CNT} given by the CNT is

$$J_{\text{CNT}} = \sqrt{2\sigma/\pi m^3}\left(\rho_v^2/\rho_l\right)\exp\left(-4\pi r_*^2\sigma/3kT\right) \tag{3}$$

where σ is the cluster surface tension, ρ_v is the vapor density, ρ_l is the cluster density, T is the vapor temperature, and r_* is the radius of the local critical cluster. Based on an extended set of experimental data, Wolk et al.[13] found that the CNT water nucleation rate over a temperature from 220 to 260 K should be corrected as a function of vapor temperature and suggested an empirical nucleation rate J_{CER} for water as follows:

$$J_{\text{CER}} = J_{\text{CNT}} \exp\{-27.56 + [(6.5 \times 10^3)/T]\} \tag{4}$$

In our work, J_{CER}, referred to as the corrected nucleation rate (CER), is extrapolated to the lower temperature region. The impact of the CER on the condensation flow will be discussed in Sec. III.

C. Collision Models

The collision process is used in the DSMC method to describe the interactions among simulated cluster and molecular particles. In addition to the monomer–monomer collision process, we must include two new types of collisions to simulate condensation plumes: cluster–monomer (C–M) and cluster–cluster (C–C) collisions. The outcome of the C–M or C–C collisions could be sticking or nonsticking.

For the Soyuz plume to be discussed in Sec. III, the only species that can condense are water and CO_2. Because the CO_2 species mole fraction in the plume is only about 5% (Table 1), it is reasonable

Table 1 Plume species, mole fractions at the nozzle exit, critical temperature T_c, and vibration characteristic temperature Θ_v

Species	Mole fractions	T_c, K	Θ_v, K
H	0.0093	31.0	——
N_2	0.2675	126.2	2256
NO	0.0012	179.8	2719
H_2	0.1905	33.0	6159
CO	0.1896	132.0	3103
CO_2	0.0524	304.2	945
H_2O	0.2895	647.0	2290

to assume that only water molecules may stick with water clusters during C–M collisions, whereas collisions between other gas species and water clusters can be modeled as nonsticking collisions. Based on MD simulations, a general expression of the collision sticking probability between a water surface and a water molecule, q, has been summarized as[26]

$$q = \left(1 - \sqrt[3]{V_l / V_g}\right) \exp(-\Delta E / kT) \tag{5}$$

where V_l and V_g are the specific volumes of gas and liquid and ΔE is the energy difference between the condensed and vapor molecules. Equation (5) shows that sticking probability is close to unity in the low-temperature region and decreases as the temperature increases. However, the sticking probabilities for small clusters may not agree well with the prediction of Eq. (5) because it is based on the condition of a macroscopic liquid surface.

The MD method was used in Ref. 14 to simulate C–M sticking probabilities as a function of collision impact parameter, collision relative velocity, and cluster size. It was found that the sticking probability increases rapidly for a cluster size less than 11-mers, whereas it remains constant, close to unity, for larger clusters. Note that n-mers refers to a cluster of n molecules. We choose Eq. (5) to calculate the sticking probabilities for all clusters in the DSMC simulations considered here because we will show that small clusters grow mainly through C–C coalescence processes rather than C–M sticking collisions. As will be discussed in Sec. III, the sticking probabilities for the collisions between small clusters and water vapor molecules have almost no impact on the condensation plume.

In previous work,[11] the C–C collisions had almost no impact on the DSMC simulation results, due to the small cluster number density in the rocket plume. However, the use of the corrected CER rate instead of the CNT nucleation rate may increase the cluster number density by about three orders of magnitude, which makes the C–C collisions more important. In this work, the semi-empirical Ashgriz–Poo model[27] is chosen to predict the outcome of C–C collisions based on impact parameter, ratio of cluster size, and Weber number. The Weber number We defined as the ratio of collision kinetic energy to cluster surface energy, is given by

$$We = \rho_c d_i c_r^2 \big/ \sigma_c \tag{6}$$

where ρ_c is the cluster density, d_i is the diameter of the smaller cluster, c_r is the C–C collision relative velocity, and σ_c is the cluster surface tension. The Ashgriz–Poo model has been verified for water droplets by MD simulations and used to predict the outcome of droplet collisions in an inductively coupled plasma.[28] The detailed description of this model may be found in Ref. 27.

The C–M and C–C collisions are modeled here as inelastic sticking or nonsticking collisions based on the general momentum and energy conservation relationships. The details of numerical scheme and simulation techniques of the collision model are given in Ref. 11.

III. Results and Discussion

The developed DSMC approach, based on the SMILE[29] code, is applied in this work to the study of condensation process in a free-expanding plume from a rocket engine with a thrust level of several thousand newton. The example plume considered here is from the Soyuz spacecraft main engine firing at an altitude of 380 km, with stagnation pressure of approximately 350 KPa and stagnation temperature of about 3800 K (Ref. 30).

The species mole fraction at the nozzle exit is shown in Table 1. The critical temperature provides an indication of the likelihood that a gaseous species will condense. Table 1 shows that for hydrazine plume conditions considered here, water (and perhaps CO_2) is the main species that will undergo homogeneous condensation. The other species remain in the gas state because the flow temperature is higher than their critical temperatures. The DSMC method requires the elastic cross section to be specified to select collision pairs randomly. The variable hard sphere model is used to represent the cross section of gaseous species, whereas the cross section for clusters is based on the expression given in Eq. (2). The molecular vibration modes are not activated in the plume because the species vibration characteristic temperatures are much higher than the flow temperature. Therefore, the molecular vibrational energy can be neglected in the DSMC simulations. It can be estimated that the average cluster collision kinetic energy is about one order of magnitude less than the cluster surface energy; thus, the possibility of the cluster fragmentation is neglected during the collision processes. The condensation simulation results based on the CNT nucleation rate had been described in previous work[11]; the following discussions will focus on the simulation results obtained with the CER, Eq. (4).

The DSMC simulation of condensation coupled plume can be summarized as follows. The parallel two-dimensional axisymmetric DSMC scheme is applied using a computational domain of 4m × 8m with 80 × 160 cells in the radial and axial directions respectively. Each cell can be divided up to 120 subcells according to the flow gradients obtained during the simulation. The grid size is determined by the mean free path, and a time step of 2.0×10^{-7} s is used to ensure that the displacement of simulated molecules per time step is less than one cell size. Because the non-condensation region close to the nozzle exit is too dense to be modeled by the DSMC approach, the simulation begins from a starting surface which is composed of 480 segments, each with a number density of approximately 4.5×10^{21} molecules/m^3. The starting surface, upstream of the initial condensation region with a Mach number greater than 2.0, is created with the continuum solver GASP.[31] About 1,200,000 simulated gas molecules and 600,000 simulated cluster molecules are used at the steady state in the DSMC simulation. After the condensation coupled flow has reached steady state, the results are then sampled up to the 400,000th time step. The simulation takes about 48 h of computational time with 18 AMD Athlon processors of 1526-MHz CPU.

The contours of cluster number density (Fig. 1a), size (Fig. 1b), and temperature (Fig. 1c) for the condensation rocket plume are shown in Figs. 1, and the nucleation region is indicated in Fig. 1a. These contours show that cluster number density decreases beyond the nucleation region due to the expansion, coalescence, and evaporation processes, whereas the average cluster size increases due to the effects of the C–C coalescence and C–M sticking collision processes. The evaporation process has very limited impact on the clusters because the cluster temperature is so low that the evaporation rate is much smaller than the C–M collision rate. The average cluster temperature decreases due to the combined effects of the coalescence and sticking heating and evaporation and the nonsticking collision cooling process. Though the non-sticking collision process may take away extra internal energy that the cluster obtains during the condensation process, there are too few C–M collisions to equilibrate the cluster internal energy with the rarefied gas environment. Thus, the condensation flow discussed in this work exhibits a thermal nonequilibrium between clusters and monomers.

As discussed in previous work, the cluster number density predicted by the original CNT nucleation rate in the rocket plume is less than 10^{16}/m^3, about five orders of magnitude smaller than the gas number density. Because of the small cluster number density with the CNT rate, the number of C–C collisions is so small that the coalescence process can be neglected, and no significant impact of condensation on the plume was observed. However, the CER predicts a cluster number density more than three orders of magnitude higher than the CNT rate. A higher nucleation rate generates more clusters by consuming more water molecules from the plume, which increases the interactions between clusters and the ambient gas environment, and at the same time increases the number of C–C collisions.

Let us check the sensitivity of our results to the cluster coalescence process modeling using the CER. Figure 2 shows a comparison of the cluster and water number density along the plume centerline between the simulations with and without the coalescence process. Note that the dashed line in Fig. 2 represents water number density along the centerline in a plume without condensation. It can be seen that the water number density decreases rapidly at an axial position of 3.5 m, due to the initiation of nucleation and cluster growth processes. The coalescence process decreases the cluster number density by about a factor of seven compared to the corresponding

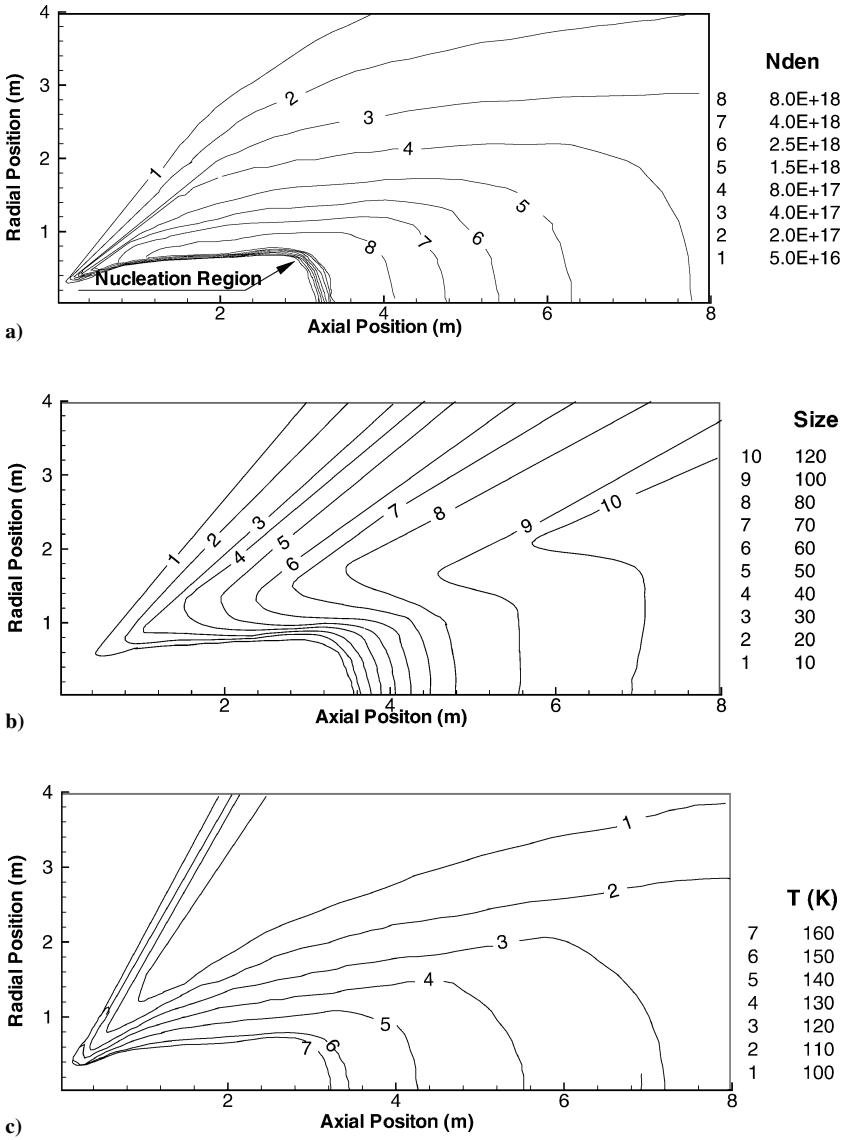

Fig. 1 Corrected CER rate with coalescence process: a) average cluster number density, b) size, and c) temperature contours.

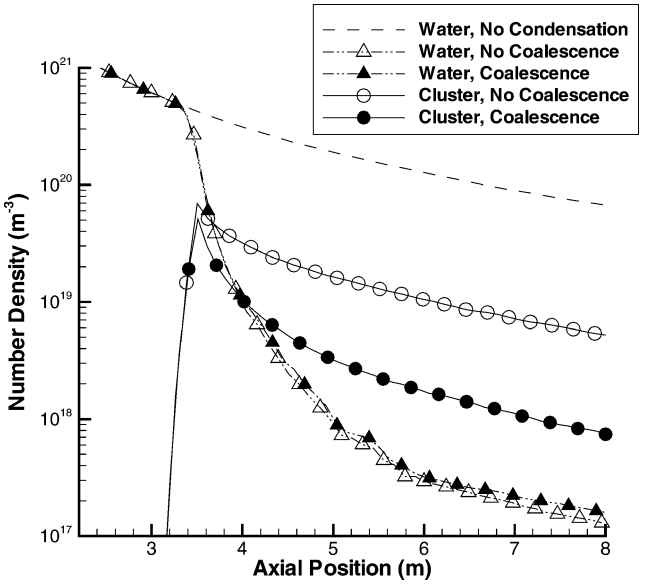

Fig. 2 Water and Cluster number density comparison for CER rate with/without cluster coalescence process along plume centerline.

no-coalescence value, but does not change the distribution of the water number density. Figure 2 suggests that the C–M sticking collision process is not important beyond 5.0 m as was the case when the CNT nucleation rate was assumed because here the water concentration is so low, on the order of $10^{17}/m^3$. Instead, when the CER is assumed, the main contribution to the cluster growth process is from the cluster coalescence process. Note that for the simulation using the original classical nucleation rate (CNT) as discussed in Ref. 11, the contribution of the coalescence process to the cluster growth could be neglected due to the small cluster number density. Figure 3 shows a comparison of the average cluster size along the plume centerline for the CER rate with and without the cluster coalescence process. Note that the dashed line in Fig. 3 is the curve of average cluster size for the original CNT rate, which was found to be the same for the simulations with and without the coalescence process. Using the CNT rate, the average cluster size continuously increases through C–M sticking collision processes beyond 15.0 m in the axial direction. Comparison of the CER rate, no-coalescence, and CER rate coalescence curves suggests that the major mechanism for cluster growth is through C–C coalescence collisions. The cluster coalescence process is the main process that accounts for the average cluster size reaching about 120-mers along the plume centerline.

The sticking probabilities for large clusters, close to unity for low-temperature conditions, have been validated by MD simulations.[26]

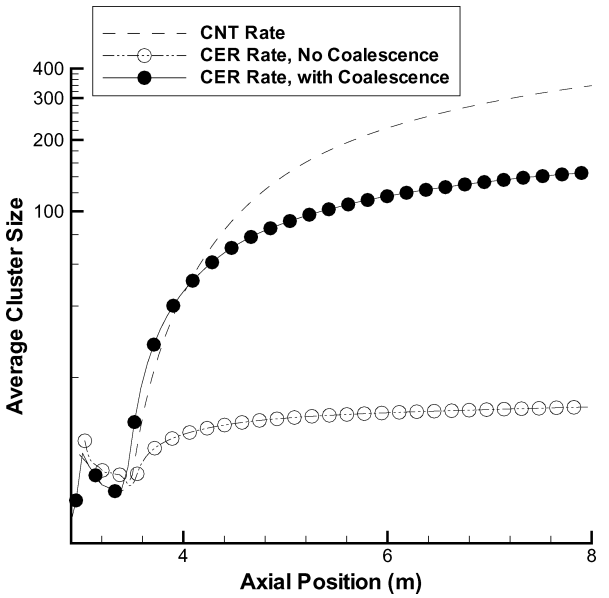

Fig. 3 Average cluster size comparison for CER rate along plume centerline, with and without cluster coalescence process.

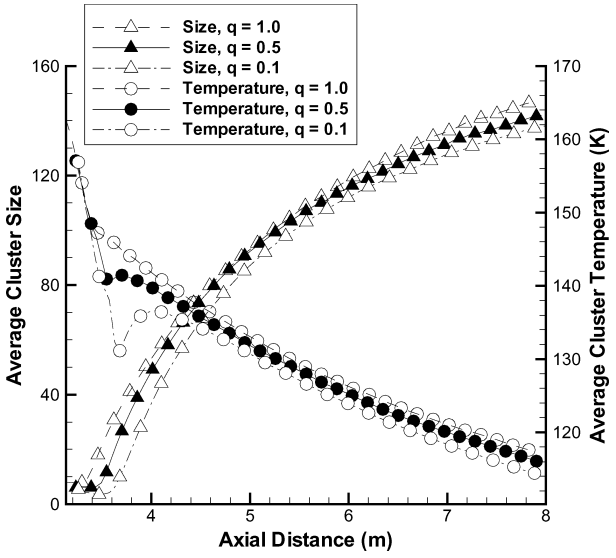

Fig. 4 Average cluster size comparison for CER rate with cluster coalescence process along plume centerline and three sticking probabilities, q, for cluster size less than 11-mers in the simulation.

However, the sticking probabilities for cluster sizes less than 11 may be quite low, as indicated by the MD simulation results in Ref. 14. To test the impact of sticking probabilities on the condensation plume, three average sticking probabilities, q, for clusters less than 11-mers are chosen for the simulations utilizing the CER rate and the coalescence process. The DSMC simulation results of cluster average size and temperature are compared along the core flow in Fig. 4. Figure 4 shows that the simulation results are insensitive to the value of the small-sized cluster sticking probabilities when the CER rate and coalescence are used in the DSMC simulation. The lack of sensitivity for these flow conditions is due to the high C–C collision frequency, which facilitates small cluster growth rapidly through the coalescence process. Also, the low water number density lessens the importance of the sticking collision process.

For the simulation with the CER rate, the number of total collisions between clusters and gas molecules increases dramatically compared with the simulation with the CNT rate. This is because a larger number of clusters exists in the simulation with the CER rate, though for each cluster the smaller cluster size tends to decrease the

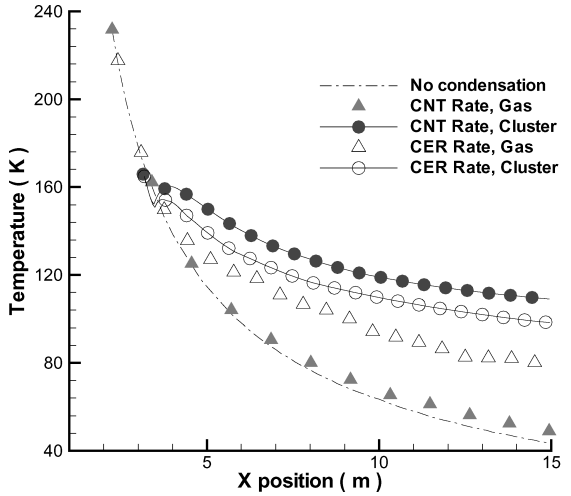

Fig. 5 Cluster and flow temperatures comparison for CER and CNT rate along plume centerline.

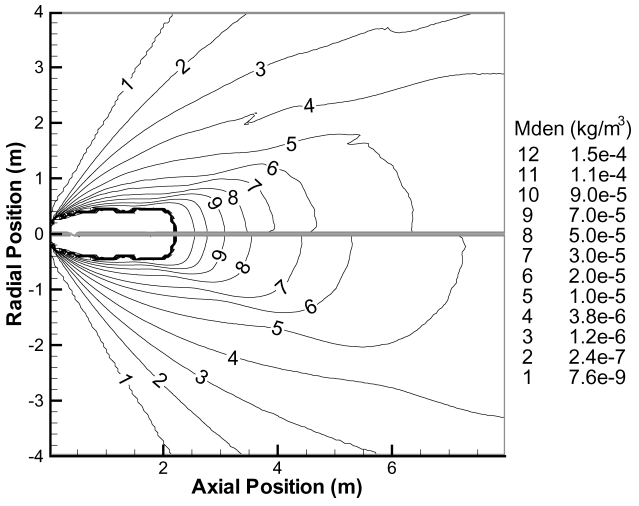

Fig. 6 Plume mass density contours comparison with condensation (top) using CER rate and flow without condensation (bottom).

number of collisions as the cluster travels through the computational domain. The latent heat released by monomers during nucleation or sticking collision process is transferred to the cluster. Subsequent collisions between clusters with plume monomers releases energy from the cluster back to the environment through nonsticking collisions. Note that in the CER vapor environment, each cluster experiences less collisions with the gas environment than with the CNT rate. Figure 5 shows a comparison of cluster and monomer temperatures along the plume centerline, the dashed line indicating the plume temperature without condensation. It can be seen that average cluster temperatures with the CER rate are lower than those with the CNT rate, whereas average flow temperatures with the CER rate are higher. Thus, the degree of nonequilibrium in the condensation flow becomes lower as the nucleation rate increases.

Finally, we want to study the impact of condensation behavior with the CER rate on the expanding plume. Note that the previous work[11] showed that there was no observable impact of condensation with the CNT rate on the plume macroparameters due to the relatively small number of clusters. Figure 6 shows a comparison of total plume gas mass density contours obtained with condensation using the CER nucleation rate (top) with a flow that does not model condensation (bottom). It can be seen that downstream of the onset of condensation, approximately at 3.6 m on the centerline, the total gas mass density in the condensation plume becomes less than the density in the plume without condensation. The reason for the decreased total gas mass density is that a large fraction of water molecules is condensed into clusters, as shown in Fig. 2. The

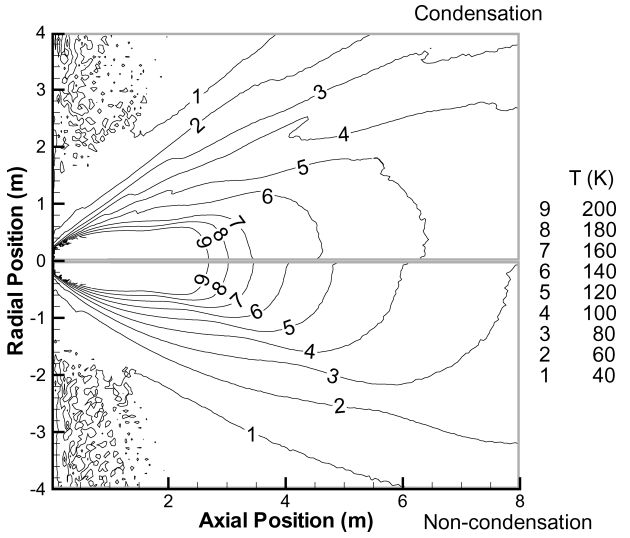

Fig. 7 Plume temperature contours comparison with condensation (top) and flow without condensation (bottom).

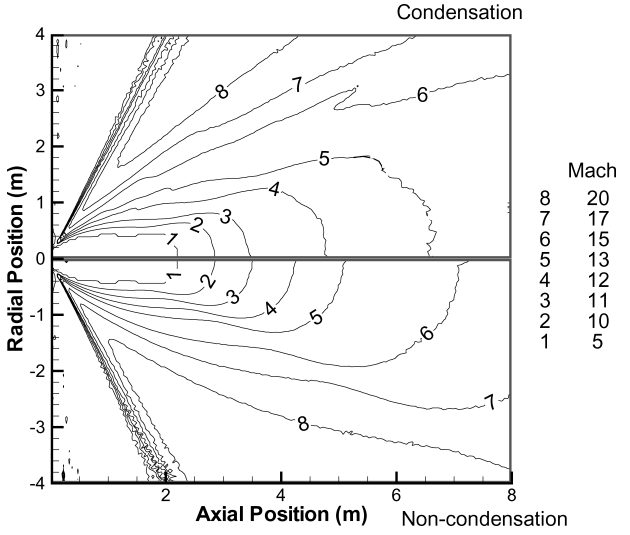

Fig. 8 Plume Mach number contours comparison with condensation (top) and flow without condensation (bottom).

comparison of plume temperature contours with and without condensation, shown in Fig. 7, indicates that the condensation process increases the plume gas temperature. The latent heat, generated during the condensation process, is released into the gas environment and increases the gas temperature. Because the maximum cluster in the condensation plume consists of hundreds of molecules, the inertia of a cluster is so small that the difference of cluster and vapor velocities, discussed in the previous work,[11] can not be seen in the condensation plume. Thus, the condensation behavior discussed in this work also does not impact the plume velocity. However, the plume sonic speed will increase due to a higher plume temperature, causing lower Mach numbers in the condensation plume as compared with those in the plume without condensation, as seen in Fig. 8. Note that the condensation process increases the plume gas temperature while decreasing the plume gas mass density. Thus, the change of total plume gas pressure in a condensation plume depends on which factor dominates. Figure 9 shows a comparison of the total gas pressure contours between the condensation (top) and noncondensation (bottom) flow, which suggests that the pressure decreases along the centerline more rapidly for the condensation vs noncondensation plume discussed in this work. Because the UV radiation observed in this hydrazine plume mainly comes from water dissociation processes, the difference in water number density distributions for a flow with and without condensation is of interest

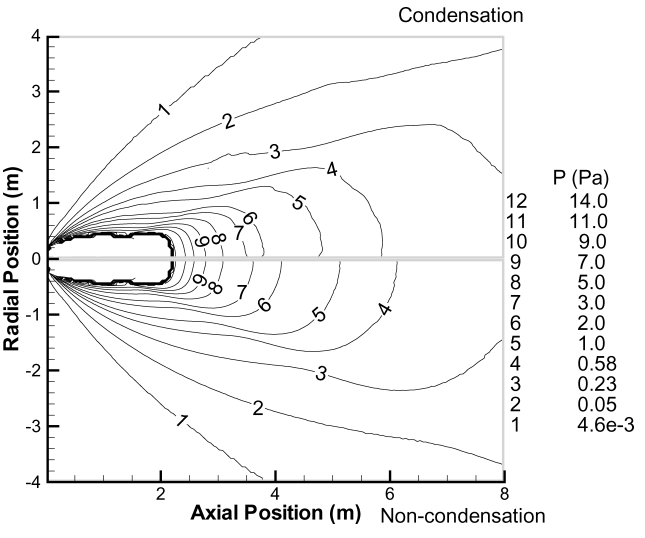

Fig. 9 Plume pressure contours comparison with condensation (top) and flow without condensation (bottom).

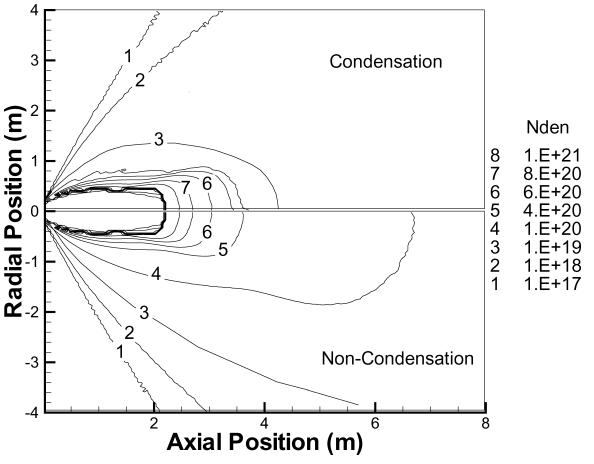

Fig. 10 Water number density comparison with condensation (top) and flow without condensation (bottom).

(Fig. 10). The data shown in Fig. 10 suggest that in a condensation plume water number density decreases more rapidly, which would also decrease water dissociation and, therefore, OH(A) UV radiation in the downstream region.

We may conclude that the CER rate has an important impact on the rocket condensation plume. The C–C coalescence is found to be important in cluster growth process for the simulation using the CER rate, whereas small cluster sticking collisions with water monomers are not important because clusters grow quickly through coalescence in a condensation plume.

IV. Conclusions

A DSMC simulation of water homogeneous condensation has been studied in a free-expansion rocket plume. A corrected semi-empirical water nucleation rate is used to model initial nuclei formation in the supersaturated vapor environment based on the CNT. The simulation results show that the condensation behavior affects the plume macroscopic flowfield and that the nucleation rate is the most important factor to impact the simulation results of a condensation flow. It can be seen that the C–C coalescence process is the main contribution to the cluster growth process.

The use of the corrected semi-empirical nucleation rate is not the only possible way to improve the accuracy of the DSMC-based kinetic approach. Another promising direction would be one based on MD characterization of possible channels for generation of initial dimers through ternary collisions, followed by implementation of

the interactions among those clusters and gas molecules in DSMC. This approach will be considered in future work.

The homogeneous condensation predicted to occur in the Soyuz plume is upstream of the region where initial water dissociation begins. As was shown in Ref. 2, the onset of water dissociation occurs when O species from the freestream is able to penetrate into the expanding plume. In the future, we will extend the computational domain shown here and combine homogeneous as well as heterogeneous water condensation and dissociation models to predict the distributions of UV radiance in hydrazine and other space plumes.

Acknowledgments

This work was supported by the Air Force Office of Scientific Research Grant F49620-02-1-0104 administered by Mitat Birkan and the Army Research Office Grant DAAD19-02-1-0196, administered by David Mann. The authors wish to express their gratitude to M. S. Ivanov for the use of the original SMILE code.

References

[1]Karabadzhak, G. F., Plastinin, Y., Afanasiev, A., Szhenov, E., Drakes, J. A., Mcgregor, W. K., Nichols, J. A., Reed, R. A., Bradley, D., Teslenko, V., Shvets, N., Volkov, O., and Kukushkin, V., "Measurements of the Progress-M Main Engine Retrofiring Plume at Orbital Conditions," AIAA Paper 99-1042, Jan. 1999.

[2]Gimelshein, S. F., Levin, D. A., Drakes, J. A., Karabadzhak, G. F., and Ivanov, M. S., "Ultraviolet Radiation Modeling from High-Altitude Plumes and Comparison with Mir Data," *AIAA Journal*, Vol. 38, No. 12, 2000, pp. 2344–2352.

[3]Abraham, F. F., *Homogeneous Nucleation Theory*, Academic Press, New York, 1974.

[4]McDonald, J. E., "Homogeneous Nucleation of Vapor Condensation I. Thermodynamic Aspects," *American Journal of Physics*, Vol. 30, No. 12, 1962, pp. 870–877.

[5]McDonald, J. E., "Homogeneous Nucleation of Vapor Condensation II. Kinetic Aspects," *American Journal of Physics*, Vol. 31, No. 1, 1963, pp. 31–41.

[6]Ivanov, M. S., Markelov, G. N., Gerasimov, Y. I., Krylov, A. N., Michina, L. V., and Sokolov, E. I., "Free-Flight Experiment and Numerical Simulation for Cold Thruster Plume," *Journal of Propulsion and Power*, Vol. 15, No. 3, 1999, pp. 417–423.

[7]Wu, B. J. C., "Possible Water Vapor Condensation in Rocket Exhaust Plumes," *AIAA Journal*, Vol. 13, No. 6, 1975, pp. 797–802.

[8]Perrel, E. R., Erickson, W. D., and Candler, G. V., "Numerical Simulation of Nonequilibrium Condensation in a Hypersonic Wind Tunnel," *Journal of Thermophysics and Heat Transfer*, Vol. 10, No. 2, 1996, pp. 277–283.

[9]Masuda, W., Satoh, M., and Yamada, H., "Effects of Water Vapor Condensation on the Performance of Supersonic Flow Chemical Oxygen-Iodine Laser," *Japan Society of Mechanical Engineers International Journal*, Series B, Vol. 39, No. 2, 1996, pp. 273–278.

[10]Bird, G. A., *Molecular Gas Dynamics and the Direct Simulation of Gas Flows*, Oxford Science, New York, 1994, p. 458.

[11]Zhong, J., Zeifman, M. I., Gimelshein, S. F., and Levin, D. A., "Direct Simulation Monte Carlo Modeling of Homogeneous Condensation in Supersonic Plumes with the DSMC Method," *AIAA Journal*, Vol. 43, No. 8, 2005, pp. 1784–1796.

[12]Hagena, O. F., and Obert, W., "Cluster Formation in Expanding Supersonic Jets: Effect of Pressure, Temperature, Nozzle Size, and Test Gas," *Journal of Chemical Physics*, Vol. 56, No. 5, 1972, pp. 1793–1802.

[13]Wolk, J., Strey, R., Heath, C. H., and Wyslouzil, B. E., "Empirical Function for Homogeneous Water Nucleation Rate," *Journal of Chemical Physics*, Vol. 117, No. 10, 2002, pp. 4954–4960.

[14]Zhong, J., Zeifman, M. I., and Levin, D. A., "A Kinetic Model of Condensation in a Free Argon Expanding Jet," *Journal of Thermophysics and Heat Transfer*, Vol. 20, No. 1, 2006, pp. 41–51.

[15]Benson, C. M., Zhong, J., Gimelshein, S. F., Levin, D. A., and Montaser, A., "Simulation of Droplet Heating and Desolvation in Inductively Coupled Plasma—Part II: Coalescence in the Plasma," *Spectrochimica Acta—Part B Atomic Spectroscopy*, Vol. 58, No. 8, 2003, pp. 1453–1471.

[16]Briehl, B., and Urbassek, H. M., "Monte Carlo Simulation of Growth and Decay Processes in a Cluster Aggregation Source," *Journal of Vacuum Science and Technology A*, Vol. 17, No. 1, 1999, p. 256.

[17]Muller, H., Fritsche, H. G., and Skala, L., "Analytic Cluster Models and Interpolation Formulae for Cluster Properties," *Clusters of Atoms and Molecules I: Theory, Experiment, and Clusters of Atoms*, edited by H. Haberland, Springer-Verlag, New York, 1995, pp. 115–138.

[18]Jorgensen, W. L., Chandrasekhar, J., Madura, J. D., Impey, R. W., and Klein, M. L., "Comparison of Simple Potential Functions for Simulating Liquid Water," *Journal of Chemical Physics*, Vol. 79, No. 2, 1983, pp. 926–935.

[19]Carravetta, V., and Clementi, E., "Water–Water Interaction Potential: An Approximation of the Electron Correlation Contribution by a Functional of the SCF Density Matrix," *Journal of Chemical Physics*, Vol. 81, No. 6, 1984, pp. 2646–2651.

[20]Dang, L. X., and Chang, T., "Molecular Dynamics Study of Water Clusters, Liquid, and Liquid–Vapor Interface of Water with Many-Body Potential," *Journal of Chemical Physics*, Vol. 106, No. 19, 1997, pp. 8149–8159.

[21]Keutsch, F. N., Cruzan, J. D., and Saykally, R. J., "The Water Trimer," *Chemical Review*, Vol. 103, No. 7, 2003, pp. 2533–2577.

[22]Dang, L. X., "Characterization of Water Octamer, Nanomer, Decamer, and Iodide–Water Interactions Using Molecular Dynamics Techniques," *Journal of Chemical Physics*, Vol. 110, No. 3, 1999, pp. 1526–1532.

[23]Goldman, N., and Saykally, R. J., "Elucidating the Role of Many-Body Forces in liquid Water. I. Simulations of Water Clusters on the VRT(ASP-W) Potential Surfaces," *Journal of Chemical Physics*, Vol. 120, No. 10, 2004, pp. 4777–4789.

[24]Sternovsky, Z., Horanyi, M., and Robertson, S., "Collision Cross Sections of Small Water Clusters," *Physical Review A*, Vol. 64, No. 2, 2001, pp. 023203–0230209.

[25]Svanberg, M., Ming, L., Markovic, N., and Pettersson, J. B. C., "Collision Dynamics of Large Water Clusters," *Journal of Chemical Physics*, Vol. 108, No. 14, 1998, pp. 5888–5897.

[26]Nagayama, G., and Tsuruta, T., "A General Expression for the Condensation Coefficient Based on Transition State Theory and Molecular Dynamics Simulation," *Journal of Chemical Physics*, Vol. 118, No. 3, 2003, pp. 1392–1399.

[27]Ashgriz, N., and Poo, J. Y., "Coalescence and Separation in Binary Collisions of Liquid Drops," *Journal of Fluid Mechanics*, Vol. 221, 1990, pp. 183–204.

[28]Benson, C. M., "An Advanced Model for the Determination of Aerosol Droplet Lifetime in an Inductively Coupled Plasma," Ph.D Dissertation, Dept. of Chemistry, George Washington Univ., Washington, DC, May 2002.

[29]Ivanov, M. S., Markelov, G. N., and Gimelshein, S. F., "Statistical Simulation of Reactive Rarefied Flows: Numerical Approach and Application," AIAA Paper 98-2669, June 1998.

[30]Drakes, J. A., Swann, D. G., Karabadzhak, G. F., and Plastini, Y., "DSMC Computations of the Progress-M Spacecraft Retrofiring Exhaust Plume," AIAA Paper 99-0975, Jan. 1999.

[31]General Aerodynamic Simulation Program, GASP Ver. 4.1, Computational Flow Analysis Software for the Scientist and Engineer, User's Manual, Aerosoft, Inc., Blacksburg, VA.